ISSN (Print) : 0974-6846
Indian Journal of Science and Technology, *Vol 10(45), DOI: 10.17485/ijst/2017/v10i45/110582,* December *2017* ISSN (Online) : 0974-5645

Wireless Optical Signal Availability and Link Range Analyses over Strong Fluctuating Meteorological Conditions with Case Study in Senegal

Cheikh Amadou Bamba Dath*, Aliou Niane, Modou Mbaye and Ndeye Arame Boye Faye

Laboratoire Atomes Lasers, Faculte des Sciences et Techniques, Universite Cheikh Anta Diop de Dakar (UCAD) ; cheikhamadou.dath@ucad.edu.sn, aliou94.niane@ucad.edu.sn, modou2812.mbaye@ucad.edu.sn, arame.boye@arsn.sn

Abstract

Objectives: Free-Space Optics (FSO) can provide high data rate, up to 10 Gbps. The performances of FSO systems are generally affected by weather conditions. In that paper we establish percentages of availabilities, the power margins and optimal link ranges of some FSO systems, for different strong meteorological conditions in Senegal. **Methods/Statistical Analysis**: Received signal and availability of FSO links are subjected to link distance and meteorological conditions like, clear atmosphere, rain, and sandstorm or in presence of heavy dust. In this paper we investigate the effects of weather conditions on the performance of FSO links, taking the climate of Senegal as a case study. However, the effect of turbulence induced irradiance fluctuation, varying beam divergence angle and misalignment conditions, and their impacts on the performances of the FSO systems were analyzed and estimated. Based on visibilities data recorded from 2003 to 2014, particular FSO link optimization's simulation cases were analyzed, in terms of power margin, availability and maximum distance. The results were performed by a lognormal distribution with good precision of the tests of correlations. **Findings:** Range and availability of optical link for different weather conditions are established easily and with high precision. As there is no known study on the effects of weather conditions in this country, this paper offers an attempt to analyze and identify the challenges related to the deployment and optimization of FSO systems under Senegalese's weather. **Application/Improvements:** For more flexibility, we forecast using an application programming interface to make easy use of the modeling approach by professional and academic actors. We plan to extend the study in all the cities in Senegal and for the Sahel region.

Keywords: FSO Link Margin, Geometric Losses, Link Availability, Mispointing Losses, Rain Losses, Scintillation Effects

1. Introduction

The FSO systems have similar capability to fiber optic in term of speed and bandwidth and are advantageous over fiber in terms of cost and time of deployment[1-3]. They are also useful in establishing communications systems during emergencies as well as for putting in place a back up link of existing networks[4,5].

But, Proposing FSO as reliable technology for telecommunications infrastructure development and access, we have to study their long distance availability and reliability by taking in consideration another fact which is the weather effects.

2. Materials Methods and approaches

2. 1 Modeling Power received and link margin

Free Space Optics (FSO) transmission is subject to absorption and scattering of the light due to the Earth's atmosphere. The atmospheric transmittance is obtained using the beer-Lambert's law[1,5-9]

*Author for correspondence

$$\tau(L)=\frac{P(L)}{P(0)}=e^{(-\gamma(\lambda)L)} \quad (1)$$

And $\gamma(\lambda)$ is the extinction coefficient described by

$$\gamma(\lambda)=\alpha_m(\lambda)+\alpha_a(\lambda)+\beta_m(\lambda)+\beta_a(\lambda) \quad (2)$$

The extinction is approximately taken to be equal to thus produced by the aerosols and expressed as:

$$\gamma(\lambda)=\beta_a(\lambda)=\frac{3.912}{V}\left(\frac{\lambda_{nm}}{550}\right)^{-q} \quad (3)$$

Coefficient q has been established within many experimental studies and may take the values below, subject to the visibility range and can take the following values according to KRUSE:

$$q=\begin{cases}1.6 & if \quad V>50\,km\\ 1.3 & if \quad 6km<V<50\,km\\ 0.585V^{1/3} & if \quad V<6\,km\end{cases} \quad (4)$$

The values of q are those proposed by Kruse, V is the atmospheric visibility which is measured by transmissometers and diffusiometers sensors. The visibility V (km) is defined as the distance to an object where the image contrast drops to 2% of its original value. It is measured at 550 nm, the wavelength that corresponds to the maximum intensity of the solar spectrum, and is given by the Koschmieder relation[1,5,7] below expressed:

$$V(\mathrm{km})=\frac{3.912}{\gamma_{550\,\mathrm{nm}}}$$

Where ϒ 550 nm is the extinction coefficient of the medium (atmosphere and aerosols). Figure 1 shows the simulations of Kruse three optical windows: 850, 1300 and 1500 nm.

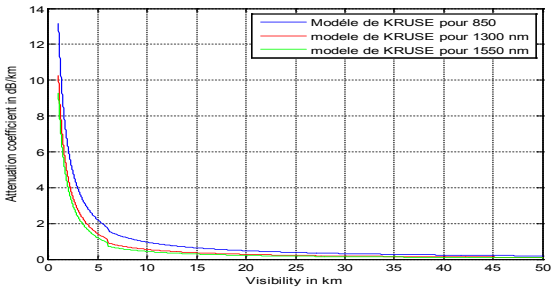

Figure 1. Kruse model profile for the windows 850, 1300 and 1550 nm.

In the model of KRUSE , it is shown that for short distance (< 500 m), the wavelength dependency of the attenuation is not significant and for longer distance link, up to 1km, the losses are wavelength dependant; It's also demonstrated that if the wavelength is big, the loss are decreasing. The link margin for a point to point link is given by the following formula[1-3,7,9].

$$M_{liaision}=P_e+|S_r|-Att_{Geo}(dB)-Att_{Atm}(dB)-P_{tot}(dB) \quad (4)$$

$$Att_{Geo}=\frac{S_L}{S_{capture}}=\frac{\frac{\pi}{4}(L\theta)^2}{S_{capture}} \quad (6)$$

$$Att_{Geo}(dB)=10\log_{10}(Att_{Geo}) \quad (7)$$

Where Pe, Sr, AttGeo AttAtm, Ptot are the emitted power, receiver sensitivity, geometric loss, atmospheric loss and system loss respectively.

The geometrical attenuation is given by:

$$\mathrm{Att\,Geo}=10\log\left(\frac{DR}{DT+d*\text{ø}}\right)^2$$

DR and DT are the diameters of the receiver and the transmitter respectively, d is the link distance in Km, θ is the beam divergence in mrad.

2.2 Data and systems used

We used visibilities data recorded during ten years, from 2004 to 2013 to estimate the range and availability of a standard FSO systems operating at 1550 nm. Extrapolations are also made for 1300 and 850 nm. The general characteristics of the system used are represented in the tabulated below with no consideration are made for tracking and non tracking capability of the system[1-3,7,9,10].

Table 1. Characteristics of FSO used for the simulation

Parameter		Comment
Average laser power	10.0 dBm	Eyes safety laser at 1550 nm, class1
System loss	-6.0 dB	Combined Tx/RX terminal losses
Geometric loss	-4.0 dB	3 mrad TX divergence; 3 mrad pointing error
Signal power on detector	-2.0 dBm	In clear air, no window loss

Detector sensitivity (Sr)	-46.0 dBm	Wavelength and data rate dependent
Aperture size (cm)	30 cm	

The parameters of the FSO systems in the e Table1 were used to prove that a 2 km link is suitable at any time. The Geometric loss related for the analysis varied between -23 and -44 dB, respectively for distance of 300 and 2,000 m; and the receiver sensitivity is around -46 dBm[3,4] .

So, for the geometric losses, we stabilize an angle of divergence limit and constant of θ= 3 mrad, when the link length is greater or equal to 2 km[1-3,7,10] .

In the system used, mispointing loss is taken into account if the link length is equal or up to 3 km[5,7,10,11].

3. Results

3.1 Analyses with compilation of visibilities data in a context of clear sky

The minimum visibility is the mean of the minimum visibility of each month along the 10 years, representing a mean value on 10 days, indicating by the way, the mean of monthly minimum visibility along all months, from 2003 to 2013.

The maximum visibility is the mean of the maximum of each month, along the 10 years, from 2003 to 2013; the mean visibility is the mean of the visibility, for each month, along the 10 years.

For the tree scenario of classification of visibilities, the corresponding extinction coefficients are calculated at 1300 nm and 1500nm and represented in the form of histograms.

By examining in Figure 2 and Figure 3, it can be seen that the values of the extinction coefficients are smaller at 1550 compared to 1300 nm; meaning by the way, that a signal will be more weakened at 1300 nm.

Also, each of the two figures can be divided into three (3) categories:

- From December to march, correspond to the first category; the extinction coefficient is the highest, this period corresponds to the lowest visibility

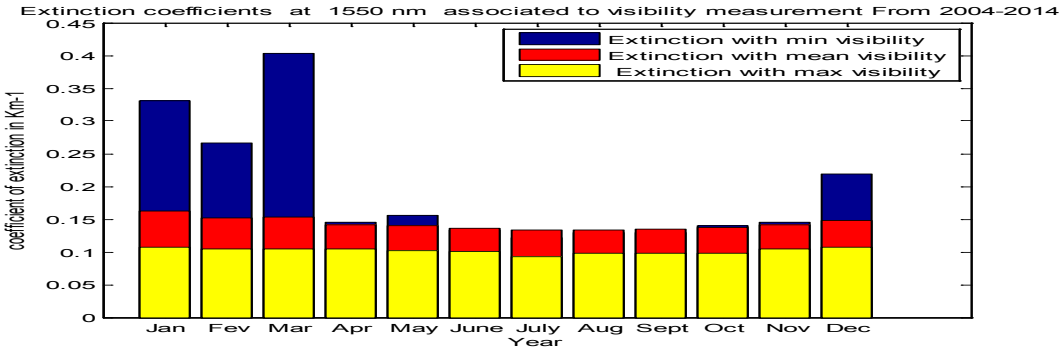

Figure 2. extinction coefficient for different visibilities at 1550 nm.

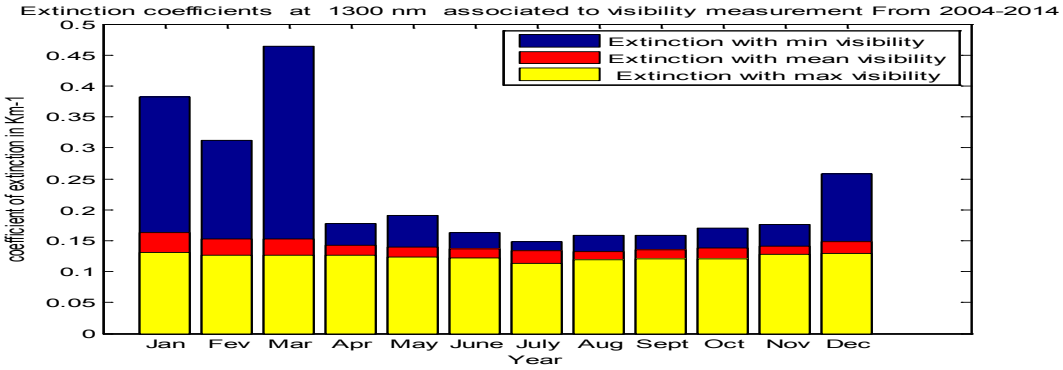

Figure 3. Extinction coefficient for different visibilities at 1300 nm.

occurrence (poorest period with max extinction in March).This period corresponds to the winter season in Dakar and the weather at this time is mostly windy, dusty.

- From April to June, corresponds to the second category. It's the dry, dusty and warm period and the visibilities are relatively highest, and are evolving increasingly until May.
- From July to November corresponds to the third category. It's the rainy season and the dust, mist and wind of strong spread do not occur. During July visibilities are greater because, clouds at low altitude are less frequent.

We determine the Probability of extinction coefficient at 1550nm, is determined, in the Figure 3.

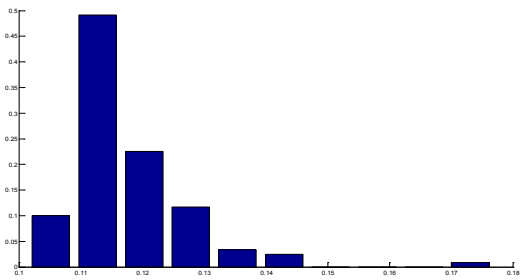

Figure 4. Probability of extinction coefficient at 1550nm.

The relative frequency meaning probability estimation of each given extinction value, could be evaluated. Also, it's possible to estimate cumulative probability for different values of extinction.

The same approach is made for the windows 1300 nm, to evaluate probability of extinction.

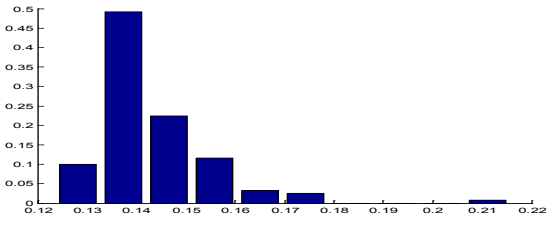

Figure 5. Probability of extinction coefficient at 1300n.

Figures 4 and 5 shows data and statistics on extinction coefficient, we can make deduction on power received, power margin. The probability of link availability, like the percentage of availability or unavailability for a given range can be estimated at 1300nm and 1500 nm.

We proceed to calculation of the power received after deduction of atmospheric losses for different extinction coefficients and for different selected ranges in km; the atmospheric losses are considered here as probabilistic losses. We also estimate the deterministic losses, which are the losses related to geometric losses, system loss and also mispoint loss. Mispointing loss is consistent when the link is up to 3 km[12].

The power profiles can easily be obtained from the extinction coefficients. However, the coefficients of extinction and the power received vary in opposite directions. The power received is obtained by simulating an FSO system with consideration of emitting power of 10 mW as mentioned in table 1.

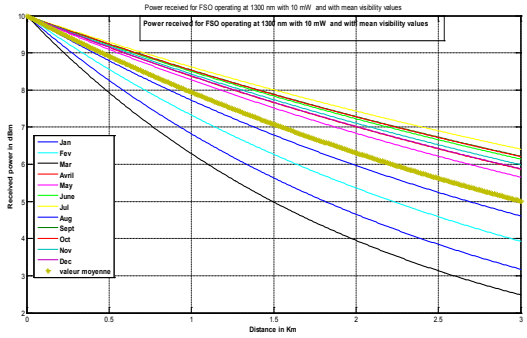

Figure 6. Monthly mean power received for FSO systems.

In the Figure 6, yearly mean of extinction coefficient at 1550nm is plotted;it shows values of extinction coefficients varying from 0.11 Km^{-1} (2009) to 0.22 Km^{1} (2013).

The transmission is: $\tau(L) = \frac{P(L)}{P(0)} = e^{(-\gamma(\lambda)L)}$,

when using the values 0.11 and.022 which are the yearly extreme's variation of the extinction coefficient, from all the period from 2004 to 2013. In that regard, the power received is expressed as, in each scenario:

$$Pr = P(L) = P(0)e^{(-\gamma(\lambda)L)} = P(0)e^{(-0.11L)}$$

$$Pr = P(L) = P(0)e^{(-\gamma(\lambda)L)} = P(0)e^{(-0.22L)}$$

To have the same ratio Pr/Pe, we have to divide the range by two (2), approximately. This means that within, days, months, hours of years, the FSO range is decreasing from distance L to L/2. In this analysis, the geometric losses and other additional constant losses related to emitting and receiving systems are not included.

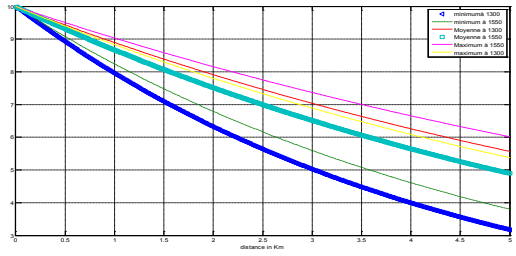

Figure 7. mean and maximum power received by FSO at 1300 &nd 1500nm.

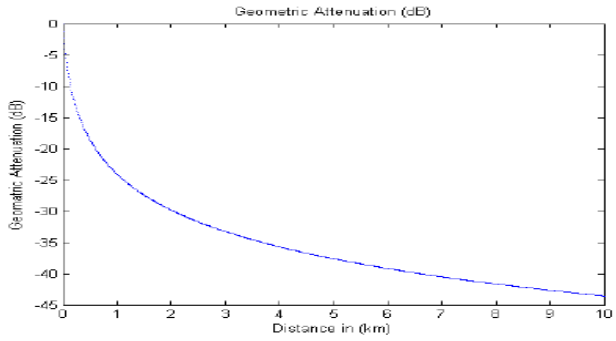

Figure 8. graphic of geometric attenuation for diverging angle of 3 mrad.

Figure 7 represents the power received at 1300 and 1500 nm, for minimum, mean and maximum visibility computed along the period from 2004-2013.

In the figure7, the minimum visibility is the worst scenario, corresponding to the highest extinction coefficient and the minimum power received. We proved that conWsidering this worse case, a link of 2 km, can be reached at any time, in Dakar[5, 6].

We know that each of daily minimum and maximum visibility in a month has the frequency of 1/30 (3,3%) and the average occurrence of visibility comprised between mean and maximum visibility are approximately 96,7%. These respective probabilities of occurrence may be considered along the all period of study.

For geometric losses, we stabilize the diverging angle not up to θ= 3 mrad, when the link reaches up to 2 km[1-3;7,10,11].

Figure 8 shows that, as link distance increases, geometric attenuation also increases, and, for example, at the distance of 5 km, the geometric attenuation is about 36 dB with angle of divergence of 3 mrad[12,13].

System losses are approximately considered to turn around 4 dB, and the pointing losses are estimated for a maximum of 4dB and are taken into consideration if the link length in up to 3 km. Table 2contains cumul of geometric and pointing losses versus link length.

By using additional provisions of Table 2, we can easily evaluate the link margin for the extinction varying from 0.22/km to 0.10/km respectively for the wavelength 1300 and 1500 nm and at a given link distance.

The respective average probabilities estimation of availability of a 5 km link with a given link margin at both 1550 and 1300 nm are resumed in the Table3.

Using elements of Table 3, we can also make a deduction of cumulative probability of link margin.

For example, the probability of availability of the link at 1500 for 0.10 < a < 0.15,by

Table 2. pointing and geometric losses cumul versus link distance

D(km)	1	2	2,2	2,4	2,6	2,8	3	3,2	3,4	3,6	3,8	4	4,2	4,4	4,6	4,8	5
Attgeo(Db)/ pointing losse	23	30	30,5	31	31,5	32	32,5	36	36,5	37	37,5	39	39,5	40	40,5	41	41,5

Table 3. availability of FSO system at 5 km range for 1300 and 1500 nm

5 KM LINK MARGIN AND AVAILABILITY												
Margin(dB)	7.82	7.61	7.39	7.17	6.95	6.74	6.52	6.30	6.09	6	5.44	5.22
A (1/km)	0.10	0.11	0.12	0.13	0.14	0.15	0.16	0.17	0.18	0.19	0.21	0.22
Availability (%) at 1300 nm	-	-	-	10	48.5	22.5	13.5	2.6	2.4	-	-	0.7
Availability (%) at 1550 nm	10	48.5	22.5	13.5	2.5	2.3	-	0.7	-	-	-	-

P (0.10 < a < 0.15) = 10+48.5+23.5+13.5+2.5+2.3 = 99.3%.

For example, the probability of availability of the link at 1300 for 0.13 < a < 0.18by

P (0.13 < a < 0.18) = 10+48.5+23.5+13.5+2.5+2.3 = 99.3%. We consider a representing the extinction coefficient.

Almost, we perform the analyses of the data by using a lognormal approximation to facilitate time and space evaluation of FSO performance for a given number, group or band of extinction coefficients.

Visibility and extinction are here phenomenon varying with time, period, and space. There are seasonal, monthly and year to year variability of these parameters: based on annual cumulative mean, annual cumulative minima and maxima, we try to establish a law governing their distribution in time and space, called a lognormal distribution.

We compute data calculated at 1500nm and 1300nm; the lognormal distribution used is expressed by the following formula:

A variable X follow a Lognormal, with parameters, μ Є R et σЄ R*+ ; α Є] α; +∞ [; if £(ln(X - α)) = N(μ ; σ 2) t Є R The corresponding probability density function is: £ (ln(X - α)) = N (μ ; σ 2) .The corresponding probability density function is:

$$f(x) = \frac{x}{(t-x')\sigma\sqrt{2\pi}} \exp\left(-\frac{(\ln(t-x')-\mu)^2}{2\sigma^2}\right) \quad (9)$$

It's usually noted that £ (X) =Log–N(α ; μ ; σ2); μ= is the shape parameter; σ is the scale parameter and x0 is the location parameter, expressed as gamma, if α=0 we will have the two parameters of the lognormal, μ ; σfor the data computed at 1500nm;Figure 9 shows a log-normal function with the parameters values hereby listed :Lognormal (3P) σ=0.40726; μ =-3.9384 α =0.09615; the number of bins use are 13.

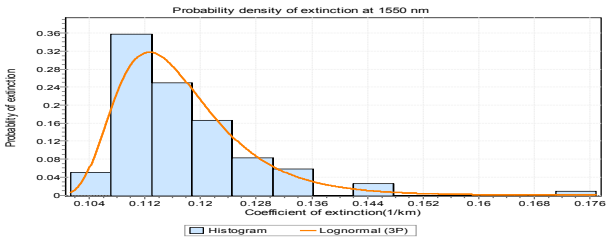

Figure 9. lognormal approximation of extinction at 1550 nm.

The Figure 9is a fit of this lognormal distribution, with 13 bins used.

And the goodness of test is established at up to 99.99% for extinction coefficient varying from 0.10/km to 0.15/km., so we can state that the probability of having 5 km link availability, at 1500nm, for specific extinction. For example, the probability of availability for given scale of extinction can be written as:

P availability (0.10<a<0.15) = 99 % and

P availability (0.10<a<0.14) = 98%

P availability (0.10<a<0.13) <= 95%

In the Figure 10, we also use a Lognormal approximation of cumulative extinction of data fitted for 1300nm with the parameters: Lognormal (3P) σ=0.40726; μ=-3.7394, α =0.11732.

Table 4. Extinction and mean visibility range for extreme dusty events condition

Time/date	26/02	27/02	28/02	01/03
00	6.6	2.2	2.3	7.4
09	8.9	4.1	2.1	4.7
12	8.6	3.3	2.3	5.3
15	8.1	2.7	2.5	5.8
18	7.9	2.1	2.7	6.5
Daily mean	8,02	2.88	2.38	5.94
Extinction 1550 nm	-	0.575137	0.733792	0.171259
Extinction 1300 nm	-	0.653002329	0.82664685	0.177576721

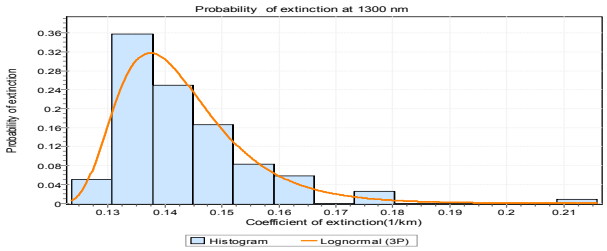

Figure 10. lognormal approximation of extinction for 1300 nm.

From Figure 10, fitting ***lognormal approximation of extinction at 1300 nm*** ,we can estimate the probability of availability at 1300 nm:

P availability (0.13<a<0.18) = 99 % and

P availability (0.13<a<0.17) = 98%

P availability (0.13<a<0.16) <= 95%

The lognormal goodness of tests for both data used in Figure 9 and 10 are evaluated using three methods: a chi-square, the kolmogorov-smirnev and Anderson- darling test, with confidence level up to 99% for both 1300 and 1500 nm. We can conclude that the lognormal with results obtained we can conclude that a 5 km link is feasible in clear sky with availability up to 99%. But to increase the availability and the quality of the service, a shorter link allowing saving a bigger power margin will be better. So a link not longer than 4 km is advised in clear sky.

3.2 Effects of Weather deep fluctuations characterized by rain and dusty events:

3.2.1 Dusty events on FSO link

In Senegal, we observe time to time dusty events and sometime over several consecutive days, mainly during the dry season, from October to June. The occurrence of dust events may cause impairment of a link[1, 14]. We investigated on the link unavailability during long term dusty events. So we will see if the link unavailability will exceed the permitted values in a given year.

In February 2015, 27th and 28th some heavy dusty events are registered in Dakar, and the daily mean visibility, decreased from 9 km to less than a mean of 2.7 km, for the two consecutive days, making by the way, severe impact on FSO link availability.

In Table 4, for all the considered scenarios, at both 1300 and 1550 nm, the minimum power received is 0.7099 mW (-1.5 dBm), after considering only atmospheric attenuation.

The additional losses (geometric losses and pointing losses) are at this range approximately 38dB. At this stage we can feasibility of a link length of 3.2 km with a margin of 6dB. The previous 5 km link foreseen is no longer possible for the whole consecutive dusty days.

So, considering that the circuits of a link need to be available approximately 99.95% for terrestrial link of the time over any consecutive 365 days, meaning, by the way, a total outage time less than 44 hours per But an availability of around 99.99 % is generally considered adequate for local loop type links where a small number of customers are dependent on the service[14].

A protecting path or a repeater is necessary when that kind of event to assure an5km link availability and to avoid an unavailability exceeding the required value per year; two days are up to 48 hr of unavailability(link outage).

3.2.2 Heavy rain attenuation and FSO link range

Rain is formed by water vapor of the atmosphere and consists of water droplets. ; they are considered as spheres for a radius of 1 mm and beyond[15,16]. Scattering due to rainfall is called non-selective scattering, this is because the radius of raindrops (100 – 1000 um) is significantly larger than the wavelength of typical FSO systems. Without consideration of the precipitation type, rainfall is characterized by space and time variable structure constituted by cells of various dimensions dependency, with speed depending on the tropospheric winds and the height of the clouds[1-3, 1,17-19].

Rain attenuation has been estimated by few methods, but the specific attenuation (dB/km) due to rain is generally approximated by the relation, for an FSO system[1,18,20]:

$$\gamma_{rain} = k \cdot R^{\alpha}$$

Another model, called Charbonneau's model, which is an empirical model depending on the rainfall rate (mm/hour), is also used for FSO rain attenuation. This model's accuracy depends on the accuracy of the rainfall rate measurements[3,7,19]. The model is given by:

$$Aattenuation(dB/Km) = 1.076 \times R^{0.67}$$

We computed the rain data from 2003 to 2013 in Dakar, to estimate the resulting effects on the FSO system.

The corresponding attenuations are derived from rain recorded. Considerations are made on rain durations, occurancies and intensities. So a lognormal approximation of the statistical analyses of the rains up to 25 mm/h, gives the curve below. In that study we consider that rain less than 25 mm/hr cannot causes serious impairments on FSO systems.

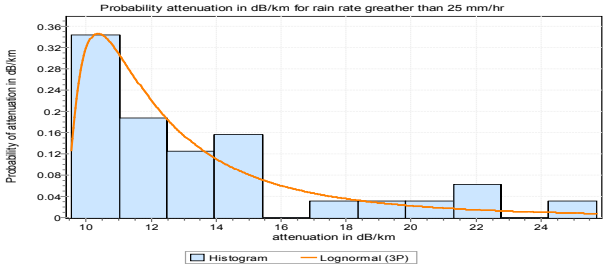

Figure 11. Probability of attenuation in dB/Km for rain rate up to 25 mm/hr.

The parameters of the lognormal function used for processing rain database in Figure 11, are:

σ =0.97796 μ =1.0293 α =9.2781

When a rain rate is greater than 25 mm/hr, we realize that the probability of having its associated attenuation in dB/km could be described by:

Probability of attenuation equal to 10dB/km is around 35% (0.35)

Probability of attenuation varying from 10dB/km to 15 dB/km is derived from the probability of rain occurrence varying from 25 to 50 mm/hr and is given by: 35% +19%+12%+15% that mean up to 81%

(0.81).The maximum attenuation calculated is 22dB/km, with a probability of occurrence smaller than 3%. Table5 gives a resume of availability analyses for different rain rates conditions.

In Table 5, we confirm that during rain events, the link range varies from a maximum of 3.2 km to 1 km for both 1300 and 1550 nm, depending on the rain rate.

This mean that a initial link length of 5 km in clear atmosphere, became under the effects of rain, a link comprised between 3.2 and 1k.

The percentage of time rain rate exceed is supposed to be 0.1 to 0.03 yearly, meaning 87 hours to 23 hours of rains. So the unavailability during rains cannot be neglected for a initial 5 km link, in clear atmosphere, but a 2 km link may be reliable with shorter link outage. The time of outage can be expressed explicitly using the table 5.

3.2.3 Scintillation effects

A second major atmospheric effect that affects the performance of FSO systems is turbulence induced atmospheric scintillation which causes deep fluctuations of the received power[20,21].

Atmospheric turbulence is occurred by presence of temporary pockets of air with small difference of temperatures, small difference of densities, and difference of

Table 5. Rain attenuation in Dakar

Rain attenuation in Dakar					
Weather condition	**Attenuation (dB/km)**	**Probability rain events occurrence**	**Maximum range(km)**	**Attenuation dB, at 1300 nm**	**Attenuation dB, at 1500 nm**
Rain of 20 mm/hr	8	-	Up to 3.2 km	1.17	1.07
Heavy rain (25 mm/hr)	9.3	Propose by UIT as A zone	2.7	1.1	0.96
rain(between 25 and 50 mm/hr)	9.3-14.8	Up to 81%	1.7-2.7	0.6978 to 1.1	0.631 to 0.96
rain(between 50 and 75 mm/hr)	14.8-19.4	Less than 9%	1.3-1.7	0.5457 to 0.6978	0.4925 to 0.631
rain(between 75 and 100 mm/hr)	19.4-23.5	Less than 10%	1.3-1	0.429 to 0.5457	0.387 to 0.4925

index of refraction. Data can be lost due to beam wander and scintillation as the laser beam becomes deformed when propagating through turbulent medium[6,19,20].

Scintillation, beam wander, beam spreading, resulting from turbulence make the beam wave front deformed and reduces the power of received signal. The effects of turbulence depend on the turbulence size; longer wavelengths will have smaller beams wander than shorter wavelengths, although the wavelength dependence is weak[5,19,21].

Tropospheric scintillations effects are generally studied from the logarithm of the amplitude χ (dB) of the observed signal ("log-amplitude"), defined as the ratio in decibels between its instantaneous amplitude and its average value. The intensity and the fluctuation rate here known as scintillation frequency increase with wavelength. For a plane wave and weak turbulence, the scintillation variance σ_x^2 (dB) can be expressed by the following relation[5,7,8,22]:

$$\sigma_\chi^2 = 23.17 \cdot k^{7/6} \cdot C_n^2 \cdot L^{11/6} \quad (8)$$

Where k is wave number (m−1), L the length of the link (m) distance between emitter and receiver, C_n^2 is the refractive index structure parameter ($m^{-2/3}$). Structure index C_n^2 is defined through next equation

$$D_n(r) = C_n^2 r^{2/3} \; l_0 \le r \le L_0 \quad (9)$$

where r is distance between measurement points of refractive index of values, the classic 2/3 power law behavior was originally suggested by Kolmogorov on the basis of dimensional analysis; n1 and n2 are refractive indexes of atmosphere in these two points and operator E represents the mean value.

The scintillations have peak amplitude of 4σχ and the attenuation due to scintillation is 2σχ. For strong turbulence, saturation of the variance given by the above relation is observed.

Attenuation due to the atmospheric turbulence αturb can be estimated from the Rytov[7,8,19,22,23] formula:

$$\alpha_{RYTOV} = 2 \cdot \sqrt{23.17 \cdot k^{7/6} \cdot C_n^2 \cdot L^{11/6}} \; . \quad \mathbf{(10)}$$

The Hufnagel-Valley model provides a model often used by researchers to describe the altitude dependence of C_n^2 (h) in rural areas. The H-V model is given by[7,8,11,13,22,25].

$$C_n^2(h) = 0.00594\left(\frac{v}{27}\right)^2 (10^{-5}h)^{10} \exp\left(-\frac{h}{1000}\right) + 2.7\times10^{-16} \exp\left(-\frac{h}{1500}\right) + A\exp\left(-\frac{h}{100}\right) \quad (11)$$

Where ν is the rms wind speed and the typical value of the parameter, $A=1.7\times10^{-14}$ $m^{-2/3}$.

C_n^2 can vary from 10^{-17} $m^{-2/3}$ up to 10^{-12} $m^{-2/3}$ for weak and strong turbulence regimes respectively.

The Table 4 below resumes the different values of Cn2, the turbulence effect on optical and radio waves propagation. Scintillation is stronger on longer optical wavelengths.

Table 6. values of C_n^2 for optical and millimeter waves

		Turbulence	
	Low (weak)	Moderate	High
Cn2 optic waves (m−2/3)	10−16	10−14	10−13
Attenuation (0.98 μm) (dB)	0.51	5.06	16.00
Attenuation (1.55 μm) (dB)	0.39	3.87	12.25

As far as we are dealing with terrestrial FSO systems; we can consider, as mentioned in Table 6, that weak turbulence values are varying from 10-16.. We also admit that turbulence is mainly occurred during rain or dusty event, so that we are going to analyze the turbulence's effect during rain events is up to 25 mm/h. We notice that in optical region, the turbulence is depending widely to the temperature variation than to the humidity variation[24,25]. And so, if rain is big, temperature tends to be uniform on the path propagation.

The calculated scintillation losses are 0.7 dB and 1.1 dB at 1550 nm, respectively for a link length of 2 km and 3 km. These values are 0.8 and 1.2 at 1300 nm, respectively for a link of 2 and 3 km.

These supplementary losses may limit the performance of a link with small margin, under rain condition equal or greater than 25 mm/hr.

4. Conclusions

In that work, we analyzed the performance of particular FSO systems, in terms of availability and link length reliability with particular emphasis of Senegalese weather conditions.

In addition, in a engineering approach, the results allow, for a given extinction coefficient, to simulated the performance of a FSO system.

The results show minimum and maximum link range at each weather condition, give by the way, a perspective

for a placement of repeaters and amplifiers for secure architecture in point to point and ring.

Otherwise, big link margin is necessary to increase the stability of FSO systems when the link range became longer than 2 km.

Conflicts of Interest: The authors declare "no conflict of interest." "The founding sponsors had no role in the design of the study; in the collection, analyses, or interpretation of data; in the writing of the manuscript, and in the decision to publish the results".

5. References

1. Bouchet O, Sizun H, Boisrobert C, Fornel FD, Favennec PN. Free-Space Optics: Propagation and Communication. Wiley-ISTE. 2006 Jan; 1–54.
2. Ghassemlooy Z, Popoola W, Rajbhandari S. Optical Wireless Communications System and Channel Modeling with MATLAB: Taylor & Francis Group. 2013; 5–38.
3. Dath CAB, Mbaye M, Arame N, Faye B, Wague A. Reliability of FSO systems in Sahel region : a case study of the major city of Dakar. International Journal of Engineering Science and Innovative Technology (IJESIT). 2015 Jan; 14(1):368–71.
4. Ijaz M, Ghassemlooy Z, Rajbhandari S, Minh HL, Perez J, Gholami A. Comparison of 830 nm and 1550nm based free space optical communications link under controlled fog conditions. Proceedings of the 8th International Symposium on Communication Systems, Networks and Digital Signal Processing (CSNDSP 12), IEEE. Poland. 2012; 1–5.
5. Almeida C, Lima M, Teixeira A. Performance analysis of 3G-UMTS WDM-RoF links. Optica Applicata. 2010; 4:773–89.
6. Son IK. Design and Optimization of Free Space Optical Networks, A dissertation thesis of the Graduate Faculty of Auburn University in partial fulfillment of the Requirements for the Degree of Doctor of Philosophy. Auburn, Alabama. 2010 Dec; 1–147.
7. Naboulsi MA. Contribution à l'étude des liaisons optiques atmosphériques, propagation, disponibilité et fiabilité, Thesis of doctorate PhD. Université de bourgogne. 2005 ; 1–209.
8. Rouissat M. Etude et Modélisation d'une Liaison Optique Sans Fil, dissertation of PhD thesis. Université Abou Bekr-Belkaid, Tlemcen, Algérie. 2013; 1–159.
9. Korevaar E, Kim II, McArthur B. Atmospheric propagation characteristics of highest importance to commercial free space optics, in Proceedings International Congress of Mathematicians. 2003 Apr; 4976(1):1–12. Crossref
10. Al-Gailani SA, Mohammad AB, Shaddad RQ. Enhancement of free space optical link in heavy rain attenuation using multiple beam concept. Optik. 2013; 124(21):4798–801. Crossref
11. Free space optical technology overview. Available from: http://www.lightpointe.com/free-space-optics-technology-overview.html.Date accessed: 18/09/2016.
12. Kim II, McArthur B, Korevaar E. Comparison of laser beam propagation at 785 nm and 1550 nm in fog and haze for optical wireless communications, Proceeding of SPIE. 2001; 4214:26–37. Crossref
13. Fixed service applications using free pace optical links. Available from: http://www.itu.int/pub/R-REP-F.2106-1-2010. Date accessed: 18/09/2016.
14. Fadhil JHA, Amphawan A, Shamsuddin HAB. Optimization of free space optics parameters: an optimum solution for bad weather conditions. Optik. 2013; 124(19):3969–73. Crossref
15. Al Naboulsi M, Sizun H, Fornel F. Fog attenuation prediction for optical and infrared waves. Journal of SPIE, Optical Engineering. 2004; 43:319–29. Crossref
16. Characteristics of precipitation for propagation modeling. Available from: https://www.itu.int/rec/R-REC-P.837-6-201202-I/en. Date accessed:22/12/2016.
17. Sharma V, Kaur G. High speed, long reach OFDM-FSO transmission link incorporating OSSB and OTSB schemes. Optik. 2013; 124(23):6111–4. Crossref
18. Kruse PW, Glauchlin LD, Mc Quistan RB. Chap 4, Element of infrared technology: Generation, transmission and detection J. Wiley and sons, New York, USA. 1962.
19. Ijaz M, Ghassemlooy Z, Pesek J, Fiser O, Le Minh H, Bentley E. Modeling of fog and smoke attenuation in free space optical communications link under controlled laboratory conditions. Journal of Lightwave Technology. 2013; 31(11):1720–6. Crossref
20. Kvicera V, Grabner M, Fiser O. Long-Term Propagation Statistics and Availability Performance assessment for Simulated Terrestrial Hybrid FSO/RF System, EURASIP Journal on Wireless Communications and Networking. 2011; 9 pp. PMid:21369160
21. Wang J, Kahn JM. Acquisition in short-range free-space optical communication, Proceedings of the SPIE Optical Wireless Communications. 2002; 4873:121–32. Crossref
22. Ryer A. Handbook: Light Measurement Handbook, International Light Inc. International Light, 17 Graf Road, Newburyport, MA 01950, USA. 1998.
23. Refai HH, Sluss JJ, Refai HH. The transmission of multiple RF signals in free-space optics using wavelength division multiplexing. Proceedings of the SPIE. USA. 2005; 5793:136–43. Crossref

24. Harris A. A free-space optical communications link to an unmanned aerial vehicle, A dissertation submitted to the graduate faculty In partial fulfillment of requirements for the degree of doctor of philosophy. Norman, Ok. 2005; 1–226.

25. Weichel H. Laser Beam propagation in the atmosphere. SPIE Press book. Bellingham, Washington, USA. 1990.